RSC Advances

ROYAL SOCIETY OF CHEMISTRY

www.rsc.org/advances

Graphical Abstract

Lamellar azobenzene–siloxane hybrids were prepared by self-directed assembly of three types of precursors where mono-, di- and triethoxysilyl groups are bridged by azobenzene groups with propylene linkers.

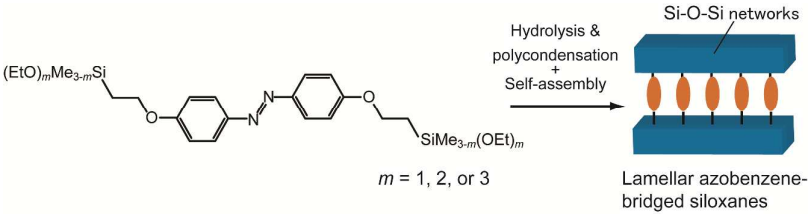

Journal Name

RSCPublishing

ARTICLE

Azobenzene–siloxane hybrids with lamellar structures from bridged-type alkoxysilyl precursors†

Cite this: DOI: 10.1039/xoxxoooooox

Sufang Guo,[a] Watcharop Chaikittisilp,[a] Tatsuya Okubo[a] and Atsushi Shimojima[b,]*

Received ooth January 2012,
Accepted ooth January 2012

DOI: 10.1039/xoxxoooooox

www.rsc.org/

Lamellar azobenzene–siloxane hybrids were prepared by controlled hydrolysis and polycondensation of three types of precursors, where azobenzene is sandwiched by mono-, di- and triethoxysilyl groups using propylene linkers. All precursors underwent reversible and fast *trans–cis* isomerization upon UV/Vis irradiation in dilute solutions. Upon hydrolysis of the triethoxysilylated precursor in a homogeneous solution under acidic conditions, precipitation occurred by self-assembly of hydrolyzed monomers into a lamellar structure. Although di- and mono-ethoxysilylated precursors produced less ordered products under identical conditions, highly ordered lamellar films were obtainable either by evaporation induced self-assembly of the hydrolyzed monomers or by solid-state reactions of precursor films. The degree of *trans–cis* isomerization of azobenzene moieties in the hybrid films was enhanced by decreasing the cross-linking degree of siloxane networks using precursors with less condensable alkoxy groups.

1. Introduction

Constructing inorganic–organic hybrid nanoarchitectures requires the integration of inorganic and organic building blocks in molecular or nanometer-length scales.[1,2] Organosiloxane is an excellent example of such hybrid materials, possessing the benefits of siloxane networks, such as good thermal/chemical stabilities and high transparency, along with diverse functionalities endowed by organic moieties. The preparation of organosiloxane-based materials with unique properties, structures and morphologies has been widely studied.[2–4]

Sol–gel hydrolysis and polycondensation of organoalkoxysilanes provides a convenient route to obtaining organosiloxane hybrids; however, this process generally yields hybrids with amorphous structures. In recent years, careful precursor designing and optimization of the reaction conditions have produced organosiloxane hybrids with ordered structures, such as lamellar and two-dimensional hexagonal structures. Organoalkoxysilanes with pendant and bridging organic (R) groups ($R–Si(OR')_3$ and $(R'O)_3Si–R–Si(OR')_3$, respectively) are commonly used. The components of organic moieties (R) are extremely important for self-assembly and therefore to direct the formation of ordered structures. Non-covalent interactions, such as hydrophobic interactions, strong H-bonds (*e.g.* urea and amide linkages) and π–π stacking interactions, often favour self-directed assembly.[5–12] In general, bridge-type precursors have the ability to incorporate a wider variety of organic groups in the siloxane networks, providing greater opportunities to create novel functional hybrid materials.

Azobenzene is a typical photo-responsive molecule that undergoes photochemical conversion between *trans* and *cis* isomers, accompanied by large changes in molecular shape and size. The arrangement and mobility of azobenzene critically influence the photo-responsive properties of azobenzene-containing materials. Azobenzene–siloxane hybrids, produced by self-directed assembly of azobenzene-containing alkoxysily precursors, are a potential new class of photo-responsive materials; however, their synthesis and properties have not yet been fully investigated. Liu *et al.* reported the synthesis of a photoactive azobenzene-bridged alkoxysilane containing urea (–NH–CO–NH–) linkages.[13] This precursor can self-assemble into lamellar structures through H-bonding interaction between urea groups and π–π interaction between azobenzene groups. However, *trans–cis* isomerization is almost inhibited in the solids possibly due to intense H-bonds. Azobenzene-bridged alkoxysilanes containing simple alkylene linkers are worth investigating as a means of improving their photo-responsive properties. Such precursors were used to produce photo-responsive mesoporous silica, where azobenzenes were randomly arranged in the pore walls, by surfactant-directed self-assembly with additional silica source.[14,15] As yet, their self-directed assembly, as well as photo-responsive properties of the products, are unexplored.

In this study, ordered azobenzene–siloxane hybrid materials were prepared by self-directed self-assembly of azobenzene-bridged alkoxysilanes containing propylene linkers. Three types of precursors with tri-, di- and mono-ethoxysilyl groups (**1**, **2** and **3** in Scheme 1) were used to study the effects of i) the number of Si–OH groups on self-assembly and ii) the degree of Si–O–Si cross-linking on photo-isomerization of bridged azobenzene groups. Powder samples (**P1**, **P2** and **P3**) were obtained as precipitates by acid-catalyzed hydrolysis and polycondensation in THF/H_2O solutions. Furthermore, to ensure high-efficiency light absorption,[13,16–21] thin films were prepared on glass substrates by either an evaporation induced self-assembly (EISA) technique (**F2** and **F3**) or solid-state reactions (**F1'**, **F2'** and **F3'**). The *trans–cis* isomerization of azobenzene groups in hybrid thin films upon UV/Vis irradiation was investigated.

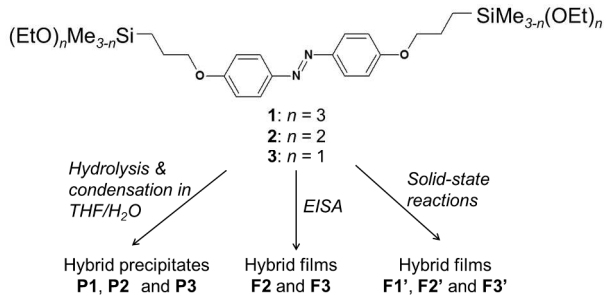

Scheme 1 Structures of bridged-type **1**, **2** and **3** precursors and the preparation pathways of hybrid powders and films.

2 Experimental

Materials

Allyl bromide (>98.0%), 4-aminophenol (>98.0%), phenol (>99.0%), sodium nitrite (>98.5%), hydrochloric acid (HCl, 1 M), sodium hydroxide (NaOH, >97.0%), N,N-dimethylformamide (DMF, dehydrated, >99.5%), ethyl acetate (>99.0%) and dimethylethoxysilane were purchased from Wako Pure Chemical Industry. Sodium hydride (NaH) (60% dispersion in paraffin liquid), triethoxysilane (>97.0%) and diethoxymethysilane (>95%) were purchased from Tokyo Chemical Industry. Platinum (0)-1,3-divinyl-1,1,3,3-tetramethyldisiloxane complexes in xylene (Pt ~2%), sulfamic acid (≥99.5%) and acetic acid (≥99.5%) were purchased from Sigma-Aldrich. All chemicals were used as received, without further purification.

Synthesis of 4,4'-dihydroxyazobenzene

The procedure was conducted as per a previous report,[22] with slight modification. 4-Aminophenol (2 g, 18.3 mmol) and 16% HCl (8.4 mL) were added to a 20 mL flask (flask A). After being stirred for 45 min at room temperature, the mixture was cooled to 0 °C. Then, a 2 M $NaNO_2$ solution was slowly added while stirring at 0 °C. The mixture was stirred at 0 °C for another 2 h, followed by the addition of sulfamic acid to remove the excess $NaNO_2$. In a 50 mL flask (flask B), phenol (1.72 g, 18.3 mmol) was mixed with a 2 M NaOH solution (1.47 g, 36.6 mmol in 17 mL H_2O). The solution in flask A was then added to flask B, and subsequently stirred at room temperature for 10 h. The crude product was recrystallized in an EtOH/H_2O solution (1:5 v/v), yielding a 1.56 g dark red product (40% yield). ^{1}H NMR (δ, 270 MHz, DMSO-d_6): 6.89–6.93 (d, 4H, Ar*H*), 7.70–7.80 (d, 4H, Ar*H*), 10.13 (s, 2H, Ar–O*H*). ^{13}C NMR (δ, 67.8 MHz, DMSO-d_6): 115.76, 124.12, 145.25, 159.96.

Synthesis of 4,4'-diallyloxyazobenzene

In a 100 mL Schlenk flask, 4,4'-dihydroxyazobenzene (1.00 g, 4.66 mmol) was dissolved in 10 mL of DMF. Activated NaH (0.56 g, 14.0 mmol), dispersed in DMF (20 mL), was added to the flask. After stirring at room temperature for 2 h, allyl bromide (3.49 g, 11.7 mmol) was added, and the mixture was stirred at 60 °C for 1 day under nitrogen atmosphere. The product was extracted with ethyl acetate, washed with cold water and dried over $MgSO_4$. Evaporation of ethyl acetate gave a dark red, crude solid product. Yellow crystals (0.64 g; yield of 47%) were obtained after recrystallization from ethyl acetate. ^{1}H NMR (δ, 270 MHz, $CDCl_3$): 4.60–4.61 (d, 4H, ArOCH_2), 5.30–5.48 (m, 4H, CH_2=CH), 6.10–6.15 (m, 2H, ArCH$_2$=C*H*), 6.98–7.04 (d, 2H, Ar*H*), 7.84–7.89 (d, 2H, Ar*H*). ^{13}C NMR (δ, 67.8 MHz, $CDCl_3$): 69.04, 114.94, 118.00, 124.33, 132.87, 147.18, 160.60.

Synthesis of 4,4'-[3-(triethoxysilyl)propoxy]azobenzene (1)

Hydrosilylation of 4,4'-diallyloxy-azobenzene (0.294 g, 1.00 mmol) in an excess amount of triethoxysilane (3.28 g, 20.0 mmol) was performed in toluene (20 mL) in the presence of a Pt catalyst (0.027 g, 2 × 10^{-5} mol). The mixture was stirred at 70 °C for 24 h under nitrogen atmosphere, and the solvent and unreacted triethoxysilane were removed *in vacuo*. **1** was obtained as red crystals (0.529 g, yield of 85%) after purification using gel permeation chromatography (GPC), with chloroform as the eluent. ^{1}H NMR (δ, 270 MHz, $CDCl_3$): 0.76–0.82 (m, 2H, OCH$_2$CH$_2$CH_2Si), 1.21–1.26 (m, 9H, Si(OCH$_2$CH_3)$_3$), 1.78–2.00 (m, 2H, OCH$_2$CH_2CH$_2$Si), 3.81–3.89 (m, 6H, Si(OCH_2CH$_3$)$_3$), 4.00–4.05 (m, 2H, OCH_2CH$_2$CH$_2$Si), 6.96–7.00 (d, 2H, Ar*H*), 7.83–7.88 (d, 2H, Ar*H*). ^{13}C NMR (δ, 67.8 MHz, $CDCl_3$):6.50, 18.32, 22.77, 58.46, 70.13, 114.67, 124.30, 146.95, 161.11. ^{29}Si NMR (δ, 53.45 MHz, $CDCl_3$): −45.53. ESI-MS: *m*/*z*: 645.2994 [M + Na]$^+$.

Synthesis of 4,4'-[3-(diethoxymethylsilyl)propoxy]azobenzene (2)

The chemical 4,4'-diallyloxyazobenzene (0.294 g, 1.00 mmol) dissolved in toluene (15 mL) was mixed with diethoxymethylsilane (2.68 g, 20.0 mmol) and 0.02 g (2 × 10^{-5} mol) of a Pt catalyst. The mixture was stirred under nitrogen atmosphere at 70 °C for 24 h. Yellow crystals (0.51 g, yield of 90%) were obtained after solvent evaporation, followed by purification using GPC. ^{1}H NMR (δ, 270 MHz, $CDCl_3$): 0.163 (s, 3H, SiCH_3), 0.74–0.80 (m, 2H, OCH$_2$CH$_2$CH_2Si), 1.20–1.28 (m, 6H, Si(OCH$_2$CH_3)$_2$), 1.75–1.95 (m, 2H, OCH$_2$CH_2CH$_2$Si), 3.75–3.83 (m, 4H, Si(OCH_2CH$_3$)$_2$), 3.98–4.03 (m, 2H, OCH_2CH$_2$CH$_2$Si), 6.95–7.01 (d, 2H, Ar*H*), 7.83–7.89 (d, 2H, Ar*H*). ^{13}C NMR (δ, 67.8 MHz, $CDCl_3$): −4.87, 9.96, 18.42, 22.82, 58.19, 70.36, 114.67, 124.30, 146.96, 161.08. ^{29}Si NMR (δ, 53.45 MHz, $CDCl_3$): −5.08. ESI-MS: *m*/*z*: 585.2786 [M + Na]$^+$.

Synthesis of 4,4'-[3-(ethoxydimethylsilyl)propoxy]azobenzene (3)

4,4'-Diallyloxy-azobenzene (0.294 g, 1.00 mmol) dissolved in toluene (15 mL) was mixed with diethoxymethylsilane (2.08 g, 20.0 mmol) and 0.02 g (2 × 10^{-5} mol) of a Pt catalyst. The mixture was stirred under nitrogen atmosphere at 70 °C for 24 h. Yellow crystals (0.43 g, yield of 85%) were obtained after solvent evaporation, followed by purification using GPC. ^{1}H NMR (δ, 270 MHz, $CDCl_3$): 0.151 (s, 6H, Si(CH_3)$_2$), 0.71–0.77 (m, 2H, OCH$_2$CH$_2$CH_2Si), 1.18–1.23 (m, 3H, SiOCH$_2$CH_3), 1.82–1.93 (m, 2H, OCH$_2$CH_2CH$_2$Si), 3.65–3.68 (m, 2H, SiOCH_2CH$_3$), 3.99–4.04 (m, 2H, OCH_2CH$_2$CH$_2$Si), 6.97–7.01 (d, 2H, Ar*H*), 7.84–7.88 (d, 2H, Ar*H*). ^{13}C NMR (δ, 67.8 MHz, $CDCl_3$): −2.10, 12.39, 18.57, 23.15, 58.34, 70.64, 114.67, 124.31, 146.96, 161.10. ^{29}Si NMR (δ, 53.45 MHz, $CDCl_3$): −5.08. ESI-MS: *m*/*z*: 525.2576 [M + Na]$^+$.

Preparation of hybrid powders (P1, P2 and P3)

An HCl aqueous solution was added to the THF solutions of **1**, **2** and **3**, yielding molar compositions of **1** : THF : H_2O : HCl = 1 : 50 : 15 : 0.03, **2** : THF : H_2O : HCl = 1 : 50 : 10 : 0.02, and **3**

: THF : H_2O : HCl = 1 : 50 : 10 : 0.02, respectively. The mixtures were stirred at room temperature for several hours. The resulting precipitates were collected by filtration and subsequently heated overnight at 120 °C, giving **P1**, **P2** and **P3**.

Preparation of hybrid films (F2 and F3) by EISA processes

An HCl aqueous solution was added to THF solutions of **2** and **3** (molar ratios of **2** : THF : H_2O : HCl = 1 : 100 : 10 : 0.02 and **3** : THF : H_2O : HCl = 1 : 100 : 10 : 0.005). The mixtures were stirred at room temperature for 2 h and 1 h, respectively. A portion of the mixtures was spin-coated on glass substrates to produce thin films. To induce further polymerization, the film prepared from **2** was exposed to 5 M HCl vapour for 30 min, and the film prepared from **3** was heated at 120 °C for 3 h to give **F2** and **F3**, respectively. Note that film samples cannot be obtained from **1** by this procedure due to precipitation upon hydrolysis.

Preparation of hybrid films (F1', F2' and F3') by solid-state reactions

First, crystalline thin films of precursors **1**, **2** and **3** were prepared by spin-coating (3000 rpm) their THF solutions (ca. 0.25 M) on glass substrates. Subsequently, **F1'**, **F2'** and **F3'** films were obtained by solid–liquid reactions, that is, by treating the precursor films in a 0.1 M HCl solution at room temperature for 15 days (**F1'**) and 9 days (**F2'** and **F3'**), followed by air drying.

Characterizations

Solution-state ^{1}H-, ^{13}C- and ^{29}Si-NMR spectra were recorded on a JEOL JNM-270 spectrometer at 270, 67.8 and 53.45 MHz, respectively. DMSO-d_6 or $CDCl_3$ was used as the solvent and tetramethylsilane as the internal reference**.** High resolution ESI mass analysis was carried out with a JEOL JMS-T100 CS instrument. Samples were dissolved in methanol. X-ray diffraction (XRD) patterns were obtained using a Rigaku Ultima IV diffractometer operated at 40 kV and 40 mA, with CuKα radiation (1.5406Å). The measurements were performed over a 2θ range of 2–30° at scanning speeds of 2° and 1° min^{-1} with a step width of 0.02° for precursors and hybrid materials, respectively. Fourier transform infrared (FT-IR) spectra were recorded using a JASCO FT/IR-6100 spectrometer by the KBr pellet technique. UV–Vis absorption spectra were recorded on a JASCO V-670 instrument. Morphologies of the samples were observed on a field-emission scanning electron microscope (FE-SEM, Hitachi S-900) with an accelerating voltage of 6 kV. Before observation, samples were sputter-coated with Pt. A SUPERCURE-204S UV light source (San-ei electric) with an intensity of 67–76 mW/cm^2 was employed for UV and visible light irradiation of the samples. UV cut (HOYA L-420 nm) and UV pass (HOYA U-340 nm) filters were used. Thermogravimetry (TG)–Differential thermal analysis (DTA) measurements were performed on Rigaku 8120 in helium atmosphere with a heating rate of 5 K min^{-1}.

3 Results and discussion

Characterizations of precursors 1, 2 and 3

The bridged-type precursors **1**, **2** and **3** have similar structures. They possess the same 'bridge' (organic fragment between the two Si atoms, having a length of ca. 1.9 nm) while differ in the number of ethoxy groups attached to each Si atom (3, 2 and 1 for **1**, **2** and **3**, respectively).

Powder XRD patterns of the precursors **1**, **2** and **3** are shown in Fig. 1. The first strong peaks are attributed to the diffractions from crystals in one orientation, corresponding to the *d*-spacings of 1.42, 1.70 and 1.93 nm, respectively. Differences in the *d*-spacings indicate the varying arrangement and/or orientation of the organic bridges. TG–DTA curves of **1**, **2** and **3** show endothermic peaks at *ca.* 85 °C, 60 °C and 79 °C, respectively, without weight losses (Fig. S1 in ESI†), which is attributed to the melting of the molecular crystals.

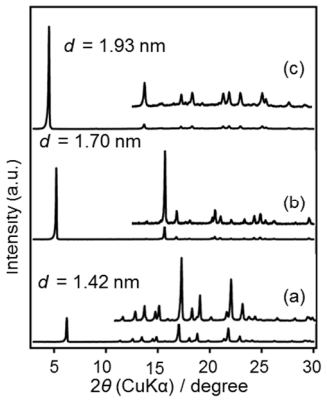

Fig. 1 Powder XRD patterns of the precursors: (a) **1**, (b) **2** and (c) **3**.

These precursors can also be obtained as thin films by spin-coating their THF solutions on glass substrates. In these films, lamellar structures are highly orientated relative to the surface, as suggested by the disappearance of diffraction peaks at high angles (Fig. S2 in ESI†). Polarized optical microscopic images of **1**, **2** and **3** films (Fig. S3 in ESI†) depict birefringent texture of crystals, indicating submicroscopic ordered structures.

The *trans–cis* photo-isomerization properties of precursors **1**–**3** were investigated by UV–Vis spectra of their dilute EtOH solutions (*ca.* 5×10^{-5} M) upon UV/Vis irradiation. As depicted in Fig. 2, all precursors before irradiation exhibited large absorption peaks at *ca.* 360 nm, due to π–π* transitions of thermally stable *trans* isomers. After 1 min of UV irradiation, the peaks significantly decreased, while the broad absorption peaks at *ca.* 440 nm due to n–π* transitions of *cis* isomers increased. A further 1 min of Vis irradiation almost recovered the spectra to the original states, in which *trans* isomers are dominant. In all cases, 1 min of UV or Vis irradiation was enough to drive azobenzenes to reach a stable isomerization state, suggesting that reversible, fast *trans–cis* photo-isomerization can be achieved in dilute EtOH solutions of **1**, **2** and **3** precursors.

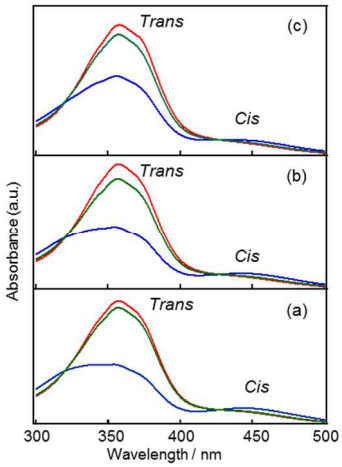

Fig. 2 UV–Vis spectra of EtOH solutions of precursors (a) **1**, (b) **2** and (c) **3**: before irradiation (red line), after 1 min of UV irradiation (blue line), and after a further 1 min of Vis irradiation (green line).

Hybrid materials prepared by hydrolysis and polycondensation of precursors 1, 2 and 3

Hybrid powders (P1, P2 and P3). FE-SEM images of **P1**, **P2** and **P3** are shown in Fig. 3. **P1** consists of plate-like particles, whereas **P2** and **P3** exhibited irregular morphologies. Powder XRD patterns of **P1**, **P2** and **P3** are shown in Fig. 4. An ordered lamellar structure with the *d*-spacing of 2.20 nm was observed for **P1**. Well-resolved diffraction peaks from the first to third order revealed the structure with a long-range order. The increased *d*-spacing, compared to the precursor crystals (*cf.* Fig. 1 and Fig. S2), may be caused by a different arrangement of the organic bridges. On the other hand, **P2** and **P3** showed a small broad peak (d = 1.66 nm) and no peak, respectively, at low 2θ regions, indicating less ordered structures with a short-range order if present. The additional peaks at higher 2θ region might be attributed to the spacings between the organic bridges and/or to some ordering in the siloxane networks,[23,24] although details are not understood.

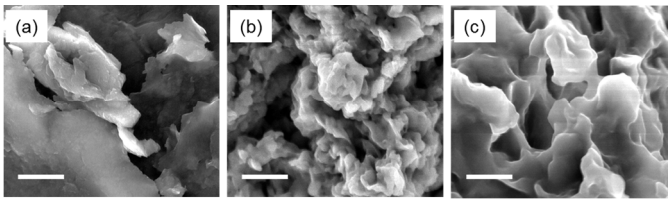

Fig. 3 FE-SEM images of (a) **P1**, (b) **P2** and (c) **P3** (Scale bar: 1 μm).

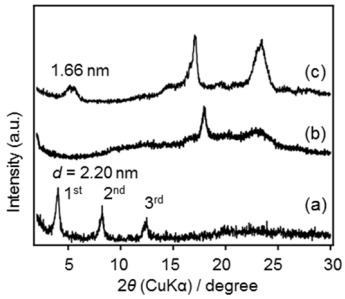

Fig. 4 Powder XRD patterns of (a) **P1**, (b) **P2** and (c) **P3**

To obtain information about the progress of hydrolysis and polycondensation, FT-IR spectra of **P1**, **P2** and **P3** were compared with those of the precursors and as-formed precipitates (*i.e.* **P1**, **P2** and **P3** before heating). The as-formed precipitates derived from **1** (Fig. 5(a, middle line)) exhibit no OCH_2CH_3 absorption peaks (2995 cm^{-1}, *cf.* Fig. 5(a, bottom line) for **1**), suggesting that the ethoxysilyl (SiOEt) groups of **1** were fully hydrolyzed. The new peak at 896 cm^{-1} was ascribed to the silanol (SiOH) groups. The large absorption band centred at *ca.* 3245 cm^{-1} can be assigned to the O–H stretching modes of SiOH and physisorbed water. No peak of isolated, free silanol groups (~3750 cm^{-1})[25] was observed. The as-formed precipitates have a highly ordered lamellar structure (Fig. S4(a), in ESI†), which is probably stabilized by H-bondings of SiOH groups.[26] After heating (Fig. 5(a, top line), the absorption bands of SiOH decreased greatly, accompanied by an increase in Si–O–Si absorption bands (*e.g.* an asymmetric stretching band of Si–O–Si at 1023 cm^{-1}). On the other hand, for **P2** and **P3**, both hydrolysis and polycondensation proceeded to a high extent even prior to heating, as judged from the intense Si–O–Si bands and relatively small SiOH bands (Fig. 5(middle lines of (b) and (c), respectively). No significant changes were observed after heating (Fig. 5(top lines of (b) and (c))

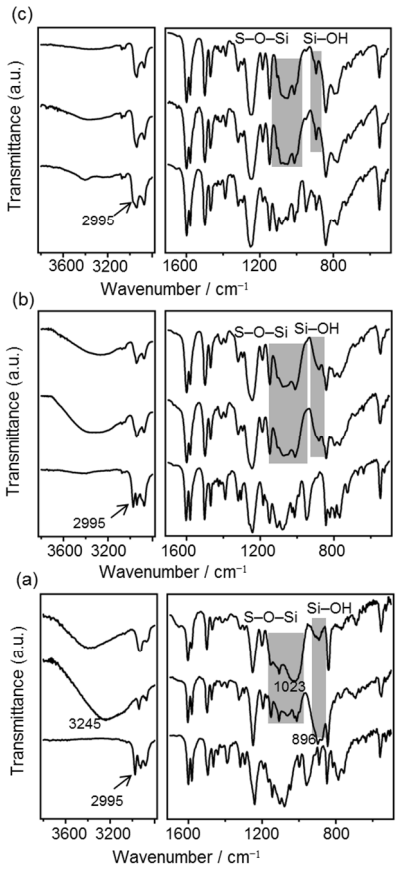

Fig. 5 FT-IR spectra of (a) precursor **1** (bottom), as-formed precipitates (middle) and **P1** (top), (b) precursor **2** (bottom), as-formed precipitates (middle) and **P2** (top) and (c) precursor **3** (bottom), as-formed precipitates (middle) and **P3** (top).

The ordered structure of **P1** was considered to be formed by self-assembly of amphiphilic hydrolyzed species through

hydrophobic (and/or π-π) interactions between organic bridges and H-bondings between silanol groups. Three steps, *i.e.* hydrolysis, self-assembly (precipitation) and polycondensation, should proceed sequentially, as supported by the above results. In the cases of less-ordered **P2** and **P3**, polycondensation likely occurred in the solutions, forming precipitates without self-assembly. The difference is attributed to the number of SiOH groups; precursors **1**, **2** and **3** can form 6, 4 and 2 SiOH groups, respectively, after complete hydrolysis. The lack of self-assembly ability of **2** and **3** may be due to the absence of adequate H-bonding interactions to stabilize lamellar structures, leading to the formation of less ordered structures.

Hybrid films (F2 and F3) prepared by EISA. EISA is a convenient method to prepare films with highly ordered mesostructures from silicate–surfactant mixtures[27,28] and hydrolyzed organoalkoxysilanes.[4,29] The preparation of a thin film from **1** by EISA was unsuccessful due to the precipitation of hydrolyzed monomers. However, **F2** and **F3** films with lamellar structures were successfully prepared by spin-coating the clear solutions containing hydrolyzed **2** and **3**, followed by HCl vapour treatment and heating, respectively, to promote polycondensation. It should be noted here that heating of as-coated **F2** caused disordering of its structure; hence, acid vapour treatment was applied instead. FT-IR spectra of these films prior to the treatment show strong SiOH peaks, suggesting as yet no obvious polycondensation (Fig. S5(b) in ESI†). This differs from their corresponding precipitates, in which no obvious SiOH bands are evident (Fig. 5, middle lines of (b) and (c)). After acid treatment or heating of these films, the SiOH bands decreased, accompanied by the appearance of Si–O–Si bands at *ca.* 1060 cm^{-1} (Fig. S5(c) in ESI†). Fig. 6 shows that **F2** and **F3** show sharp diffraction peaks due to lamellar structures with the *d*-spacings of 1.83 and 1.59 nm, respectively, in contrast to the broad peaks observed for **P2** and **P3** precipitated from the hydrolyzed solutions. It is apparent that fast evaporation of the solvents facilitated the self-assembly of hydrolyzed species prior to polycondensation. The additional small, sharp peaks (2θ = ca. 8° and 10.5°) suggest the presence of other phases, which are unidentified yet.

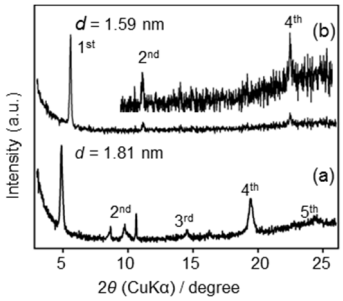

Fig. 6 XRD patterns of (a) **F2** and (b) **F3**.

Hybrid films (F1', F2' and F3') prepared by solid-state reactions. In solid-state reaction, reactive vapour or liquid diffuses into solids and subsequent hydrolysis and polycondensation reactions occur at the interface of two phases. In this process, morphologies or the ordered structures of the precursors are prone to be preserved.[30,31] The reaction may be hindered by a slow diffusion of reactive agents into solid phases, especially after siloxane formation. In this work, solid–liquid reactions of **1**, **2** and **3** precursor films in HCl aqueous solutions (0.1 M) were conducted. Reaction rates were relatively slow compared to solution-phase reactions; it was confirmed that ethoxy groups were almost eliminated after 9 days in the cases of **2** and **3** but additional 6 days were required for **1**. FT-IR spectra of **F1'**–**F3'** (Fig. S6 in ESI†) exhibited absorption peaks for Si–O–Si siloxane bonds (1060 cm^{-1}), indicating the progress of hydrolysis and polycondensation, although peaks for the SiOH (900 cm^{-1}) groups still remained to some extent.

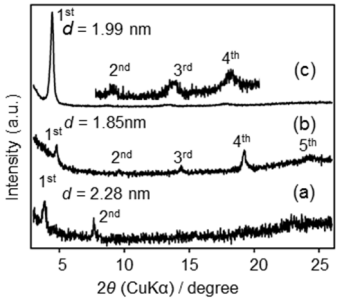

Fig. 7 XRD patterns of (a) **F1'**, (b) **F2'** and (c) **F3'**.

The XRD patterns of **F1'**–**F3'** films are shown in Fig. 7. All films showed lamellar structures, with *d* = 2.28, 1.85 and 1.99 nm for **F1'**, **F2'** and **F3'**, respectively. Relatively weak peaks in **F1'** and **F2'** indicated less ordered structures, likely due to a partial loss of the crystalline arrangement of precursor molecules during the solid-state reaction. The *d*-spacings of **F2'** and **F3'** were similar to those of the precursor films (1.89 nm and 1.93 nm, Fig. S2 in ESI†) indicating the almost unchanged molecular arrangements, despite the conversion of SiOEt to Si–O–Si.

Photo-responsive properties of the hybrid films

The photo-responsive properties of the hybrid films (**F2**, **F3**, **F1'**, **F2** and **F3'**) were investigated by measuring their UV–Vis spectra upon light irradiation. We have recently reported that azobenzene–siloxane hybrid films prepared from pendant-type precursors showed partial but reversible *trans–cis* isomerizations.[16] Bridged-type alkoxysilyl precursors may suffer from a low mobility of bridging azobenzene groups due to greater constraints at both ends, thereby limiting *trans–cis* isomerization. It is expected that a decrease in the degree of Si–O–Si cross-linking by utilizing precursors with less SiOEt groups will increase the flexibility of siloxane networks improving the mobility of azobenzene groups.

As azobenzenes are less mobile in films than in solutions, a longer time (5 min) of irradiation (1 min for solutions) was conducted. As depicted in Fig. 8(a), **F2** shows an apparent increase in absorption at 450 nm upon UV irradiation, indicating a partial of *trans* to *cis* isomerization. However, absorption at 350 nm also increased after UV irradiation, which is possibly due to an orientation change of azobenzene moieties relative to incident light caused by order–disorder transition upon irradiation, as described later. In contrast, **F3** (Fig. 8(b)) showed obviously reversible *trans–cis* isomerization upon UV/Vis irradiation, with the isomerization degree comparable to that of pendant-type hybrids.[16]

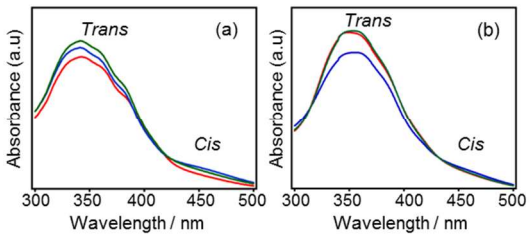

Fig. 8 UV–Vis spectra of (a) **F2** and (b) **F3** films before irradiation (red line), after 5 min of UV irradiation (blue line), and after a further 5 min of visible light irradiation (green line).

XRD patterns of **F2** and **F3** before and after UV/Vis irradiations are shown in Fig. 9. For **F2**, UV irradiation caused a disappearance of the XRD peaks and a further Vis irradiation did not recover the lamellar structure (Fig. 9(a)). This order-to-disorder transition upon UV irradiation was considered to be caused by the very small partial *trans*-to-*cis* transition of azobenzene (described as above). Further polycondensation may occur after UV irradiation, fixing the disordered structure, and thereby inhibiting a reversible change into the initial ordered structure even after Vis irradiation (Scheme S1 in ESI†). Further polycondensation after UV irradiation was confirmed by FT-IR spectra (Fig. S7 in ESI†). On the other hand, neither a change in the diffraction peak intensity nor position was observed for **F3** upon UV/Vis irradiation (Fig. 9(b)). One possible explanation is that **F3** contains some disordered domains, where azobenzene groups can more easily undergo photoisomerization.

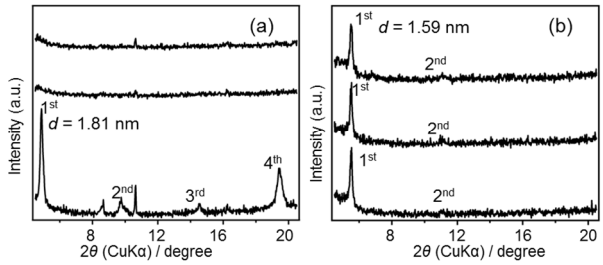

Fig. 9 XRD patterns of (a) **F2** and (b) **F3**: (bottom) before irradiation, (middle) after 5 min of UV irradiation, (top) after a further 5 min of visible light irradiation.

UV–Vis spectra of **F1'**, **F2'** and **F3'** (Fig. S8 in ESI†) show large absorption peaks for the *trans* isomers of azobenzene even after UV irradiation. There were no changes upon UV/Vis irradiation for **F1'**, which is also in clear contrast to pendant-type hybrid.[16] The absorption peak of **F1'** at 330 nm was obviously blue shifted in comparison to the ethanol solution of **1** (Fig. 2), as well as to the **F2'** and **F3'** films. This suggested an enhanced H-aggregation of azobenzene moieties.[32,33] In **F1'**, the closer packing of azobenzene groups and the more rigid siloxane networks should hinder photo-isomerization. In contrast, **F2'** and **F3'** films showed slightly reversible *trans–cis* isomerizations after UV/Vis irradiation, likely due to the lower cross-linking degree of siloxane networks. However, these changes were smaller than those observed for **F2** and **F3**, suggesting that solid-state reactions gave siloxane networks which limited the mobility of azobenzene moieties.

4. Conclusions

We have demonstrated the formation of lamellar hybrid materials from azobenzene-bridged ethoxysilane precursors. Three types of photo-responsive precursors differing in the number of ethoxy groups were used. The triethoxysilylated precursor, which generates the largest number of SiOH groups, had a strong tendency to form self-assembled, lamellar structures. By employing an evaporation induced self-assembly process or a solid-state reaction process, highly ordered lamellar structures were also prepared from di- and mono-alkoxysilyl precursors. The photo-responsive properties of the hybrid films were influenced by cross-linking degree of siloxane networks: *trans–cis* isomerization of azobenzene moieties was improved by decreasing of Si–O–Si bonds via utilizing precursors with less condensable ethoxy groups. Further structural design of such self-assembled hybrid materials will lead to the creation of novel photo-responsive materials.

Acknowledgements

The authors thank Mr. Masashi Yoshikawa (Waseda University) for his help in the ESI-MS analysis. This work was supported in part by a Grant-in-Aid for Scientific Research (C) from Japan Society for the Promotion of Science (JSPS) and by a Grant-in-Aid for Scientific Research on Innovative Areas 'New Polymeric Materials Based on Element-Blocks (No. 2401)' provided by The Ministry of Education, Culture, Sports, Science and Technology, Japan. S.G. acknowledges the financial support offered by the Monbukagakusho Scholarship and by the Global Centre for Excellence for Mechanical Systems Innovation (GMSI, The University of Tokyo).

Notes and references

[a] Department of Chemical System Engineering, The University of Tokyo, 7-3-1 Hongo, Bunkyo-ku, Tokyo 113-8656, Japan.
[b] Department of Applied Chemistry, Waseda University, 3-4-1 Ohkubo, Shinjuku-ku, Tokyo 169-8555, Japan. E-mail: shimojima@waseda.jp
† Electronic Supplementary Information (ESI) available: FigS1–S8 and Scheme S1. See DOI: 10.1039/b000000x/

1 F. Hoffmann, M. Cornelius, J. Morell and M. Froba, *Angew. Chem., Int. Ed.*, 2006, **45**, 3216.
2 a) A. Mehdi, C. Reye and R. Corriu, *Chem. Soc. Rev.*, 2011, **40**, 563, b) A. Chemtob, L. Ni, C. Croutxé-Barghorn and B. Boury, *Chem. Eur. J.*, 2014, **20**, 1790.
3 W. Chaikittisilp, M. Kubo, T. Moteki, A. Sugawara-Narutaki, A. Shimojima and T. Okubo, *J. Am. Chem. Soc.*, 2011, **133**, 13832.
4 K. Kuroda, A. Shimojima, K. Kawahara, R. Wakabayashi, Y. Tamura, Y. Asakura and M. Kitahara, *Chem. Mater.*, 2014, **26**, 211.
5 A. Shimojima, Y. Sugahara and K. Kuroda, *Bull. Chem. Soc. Jpn.*, 1997, **70**, 2847.
6 L. D. Carlos, V. D. Bermudez, V. S. Amaral, S. C. Nunes, N. J. O. Silva, R. A. S. Ferreira, J. Rocha, C. V. Santilli and D. Ostrovskii, *Adv. Mater.*, 2007, **19**, 341.
7 H, Peng, J. Tang, J. Pang, D. Chen, L. Yang, H. S. Ashbaugh, C. J. Brinker, Z. Yang and Y. Lu, *J. Am. Chem. Soc.*, 2005, **127**, 12782.
8 J. J. Moreau, L. Vellutini, M. Wong Chi Man, C. Bied, J.-L. Bantignies, P. Dieudonne and J.-L. Sauvajol, *J. Am. Chem. Soc.*, 2001, **123**, 7957.

9 J. J. E. Moreau, B. P. Pichon, M. Wong Chi Man, C. Bied, H. Pritzkow, J.-L. Bantignies, P. Dieudonne and J.-L. Sauvajol, *Angew. Chem., Int. Ed.*, 2004, **43**, 203.
10 J. J. E. Moreau, B. P. Pichon, G. Arrachart, M. Wong Chi Man and C. Bied, *New J. Chem.*, 2005, **29**, 653.
11 J. J. E. Moreau, L. Vellutini, M. Wong Chi Man, C. Bied, P. Dieudonne, J.-L. Bantignies and J.-L. Sauvajol, *Chem. Eur. J.*, 2005, **11**, 1527.
12 F. Ben, B. Boury and R. J. P. Corriu, *Adv. Mater.*, 2002, **14**, 1081.
13 N. Liu, K. Yu, B. Smarsly, D. R. Dunphy, Y.-B. Jiang and C. J. Brinker, *J. Am. Chem. Soc.*, 2002, **124**, 14540.
14 M. Alvaro, M. Benitez, D. Das, H. Garcia and E. Peris, *Chem. Mater.*, 2005, **17**, 4958.
15 E. Besson, A. Mehdi, D. A. Lerner, C. Reye and R. J. P. Corriu, *J. Mater. Chem.,* 2005, **15**, 803.
16 S. Guo, A. Sugawara-Narutaki, T. Okubo and A. Shimojima, *J. Mater. Chem. C*, 2013, **1**, 6989.
17 M.-H. Li, P. Keller, B. Li, X. Wang and M. Brunet, *Adv. Mater.*, 2003, **15**, 569.
18 T. Ikeda, M. Nakano, Y. Yu, O. Tsutsumi and A. Kanazawa, *Adv. Mater.*, 2003, **15**, 201.
19 T. J. White, N. V. Tabiryan, S. V. Serak, U. A. Hrozhyk, V. P. Tondiglia, H. Koerner, R. A. Vaia and T. J. Bunning, *Soft Matter*, 2008, **4**, 1796.
20 M. Yamada, M. Kondo, J. Mamiya, Y. Yu, M. Kinoshita, C. J. Barrett and T. Ikeda, *Angew. Chem., Int. Ed.*, 2008, **47**, 4986.
21 M. Yamada, M. Kondo, R. Miyasato, Y. Naka, J. Mamiya, M. Kinoshita, A. Shishido, Y. Yu, C. J. Barrett and T. Ikeda, *J. Mater. Chem.*, 2009, **19**, 60.
22 C. Kordel, C. Popeney and R. Haag, *Chem. Commun.*, 2011, **47**, 6584.
23 S. S. Nobre, X. Cattoen, R. A. S. Ferreira, C. Carcel, V. Z. Bermudez, M. Wong Chi Man and L. D. Carlos, *Chem. Mater.*, 2010, **22**, 3599.
24 B. Menaa, M. Takahashi, P. Innocenzi and T. Yoko, *Chem. Mater.*, 2007, **19**, 1946.
25 X. Zhou, S. Yang, C. Yu, Z. Li, X. Yan, Y. Cao, and D. Zhao, *Chem. Eur. J.* 2006, **12**, 8484.
26 G. Cerveau, S. Chappellet, R. J. P. Corriu, B. Dabiens and J. L. Bideau, *Organometallics*, 2002, **21**, 1560.
27 C. J. Brinker, Y. Lu, A. Sellinger and H. Fan, *Adv. Mater.*, 1999, **11**, 579.
28 L. Nicole, C. Boissiere, D. Grosso, A. Quach and C. Sanchez, *J. Mater. Chem.*, 2005, **15**, 3598.
29 A. Shimojima and K. Kuroda, *Chem. Rec.*, 2006, **6**, 53.
30 H. Muramatsu, R. Corriu and B. Boury, *J. Am. Chem. Soc.*, 2003, **125**, 854.
31 B. Boury, F. Ben, R. J. P Corriu, *Angew. Chem. Int. Ed.*, 2001, **40**, 2853.
32 Z. T. Nagy, B. Heinrich, D. Guillon, J. Tomczyk, J. Stumpe and B. Donnio, *J. Mater. Chem.*, 2012, **22**, 18614.
33 C. L. Yeung, S. Charlesworth, P. Iqbal, J. Bowen, J. A. Preeceb and P. M. Mendes, *Phys. Chem. Chem. Phys.,* 2013, **15**,11014.